Journal of Biomechanics 94 (2019) 67–74

Contents lists available at ScienceDirect

Journal of Biomechanics

journal homepage: www.elsevier.com/locate/jbiomech
www.JBiomech.com

Representative 3D shape of the distal femur, modes of variation and relationship with abnormality of the trochlear region

Pietro Cerveri [a], Antonella Belfatto [a], Alfonso Manzotti [b]

[a] Department of Electronics, Information and Bioengineering, Politecnico di Milano University, Milan, Italy
[b] Orthopaedic and Trauma Department, "Luigi Sacco" Hospital, ASST FBF-Sacco, Milan, Italy

ARTICLE INFO

Article history:
Accepted 9 July 2019

Keywords:
Distal femur
Trochlear region
Statistical shape model
Morphometry
Dysplasia

ABSTRACT

The anatomy of the distal femur has a predominant influence on the mechanics of both patello- and tibio-femoral joints. Especially, the morphological degeneration of the trochlear region dramatically affects the overall knee biomechanics and, from a clinical point of view, the staging of such a degeneration is fundamental to tailor the optimal therapeutic solution. The description of morphological variability and pathological inter-subject differences of the trochlea can be achieved by means of statistical shape modeling of a set of three-dimensional surfaces. This representation encodes information, spread into the dataset, in terms of modes of variations that model global, regional and even local morphological features. In view of that, the aim of this study was to develop a statistical shape model of the distal femur to capture the variability of the trochlear region into specific modes of variation and to study the interplay between the variation of the trochlea and the condylar regions. Using CT scans of patients affected by different levels of abnormality of the trochlear region, the distal femur geometries were co-registered to a reference shape using the pair-wise correspondence approach and principal component analysis provided the key modes of variation (MoVs). Apart from the first two MoVs, which described the global magnitude of the femur and the shaft length, the main following ones showed high correlation with sulcus depth ($r^2 = 0.70$), sulcus angle ($r^2 = 0.70$), lateral trochlear inclination ($r^2 = 0.66$), and height of the two condylar facets in the anterior direction ($r^2 = 0.66$), whose abnormal variations are typical signs of trochlear degeneration. High interplay between trochlear abnormalities and notch width ($r^2 = 0.71$), lateral condylar size ($r^2 = 0.67$), and medial condylar size ($r^2 = 0.99$) was found. Interestingly, the model predicted morphological associations not included in the training dataset, nonetheless difficult to demonstrate physiologically. Interestingly from a biomechanical point of view, the distribution of some MoVs was found statistically different across the patients featuring physiological and pathological ranges of hip-knee-ankle alignment, femoral internal-external rotation and tibial slope. However, no linear correlation was found between the angular indexes and such MoVs. As a result, we can assert that statistical modeling of the distal femur are to date an effective way to visualize and quantify abnormalities of the trochlear regions supporting the introduction of advanced analysis, diagnostic and treatment support tools to elucidate physiologic and pathological variability in the morphology, to drive the staging and assist the selection of the optimal treatment option tailored to the patient.

1. Introduction

The anatomy of the distal femur has a predominant influence on both patello- and tibio-femoral joints in the knee (Hing et al., 2006; Monk et al., 2014; Gillespie et al., 2015). Especially, morphological abnormalities affecting the trochlear region as dysplastic conditions are associated to early cartilage degradation leading to knee pain, increasing the risk of mechanical instability of the patello-femoral joint and making the knee potentially prone to patellar dislocation (Yamada et al., 2007; Cho et al., 2009; Jungmann et al., 2013; Dejour et al., 2014). In addition, such morphological modifications can induce instability in the mechanics of the tibio-femoral joint (Lee et al., 2003; Balcarek et al., 2013; Botchu et al., 2013b; Van Haver et al., 2015; de Lange-Brokaar et al., 2016; Iranpour et al., 2017). Consequently, the evaluation of the status of the trochlear region becomes clinically relevant for early diagnosis and, in case of degeneration, the selection of the most suitable therapeutic option including surgery, as trochleoplasty and total knee replacement (Davidson and

E-mail address: pietro.cerveri@polimi.it (P. Cerveri).

https://doi.org/10.1016/j.jbiomech.2019.07.008
0021-9290/

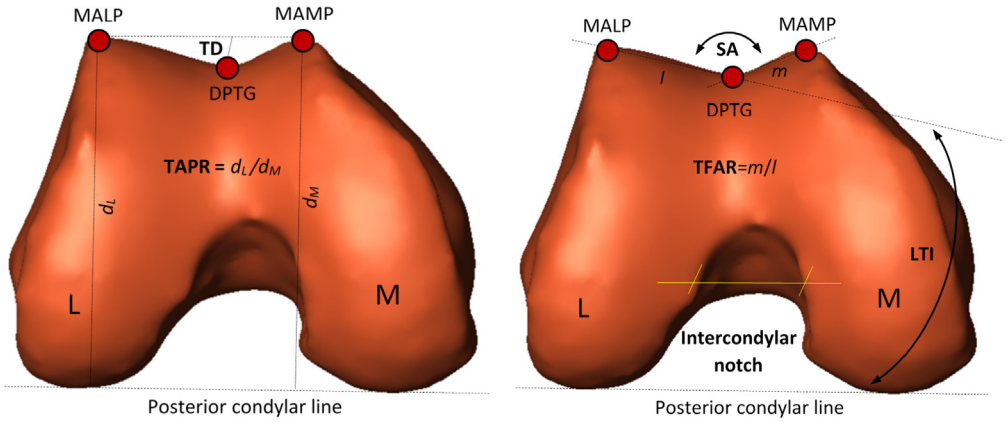

Fig. 1. Trochlear depth, sulcus angle, lateral trochlear inclination, trochlear facet asymmetry ratio and trochlear antero- posterior ratio. The quantities needs the identification of the most anterior lateral point (MALP), the most anterior medial point, deepest point on the trochlear groove in anterior direction (DTPG), and the posterior condylar line.

Rivenburgh, 2008; Nelitz et al., 2013; LaPrade et al., 2014; Song et al., 2014; Longo et al., 2017). Nonetheless, the correct diagnostic evaluation of the severity of the pathological condition and the related choice between conservative and surgical treatments still remain controversial because of the trochlear shape complexity and the morphological abnormalities of other regions in the distal femur (Biedert and Bachmann, 2009; Iranpour et al., 2010; Biedert et al., 2011; Botchu et al., 2013b; Chen et al., 2017). As a matter of fact, the trochlear geometric profile features a complex asymmetric saddle shape and its orientation, length, and curvature show a large inter-subject variability. Additionally, the morphological abnormality and concurrent damages at condylar level complicate the clinical analysis. Thereby, understanding anatomical variation and pathological degeneration at the trochlear region can provide insight into patello-femoral mechanics, assist clinicians in staging the abnormality degree, and help set screening protocols for therapeutic selection.

In order to stage the abnormality of the trochlea, the clinical practice usually exploits qualitative morphological signs, detected on radiographic images, such as the relative size and convexity of the two condylar facets, the flatness of the trochlear groove and the anteriorization of trochlear ridges (Dejour et al., 1994; Fucentese et al., 2006, 2011; Dejour et al., 2014). The lack of a gold standard makes this assessment strongly dependent on the observer interpretation, reducing the consensus about the staging (LaPrade et al., 2014; Latt et al., 2014). Quantitative methods exploit anatomical landmarks to compute geometric features of the distal femur (Fig. 1) such as the trochlear depth (TD[1]), the sulcus angle (SA[2]), the lateral trochlear inclination (LTI[3]), the trochlear facet asymmetry ratio (TFAR[4]) and the trochlear anterior-posterior ratio (TAPR[5]) (Pfirrmann et al., 2000; Escala et al., 2006; Fucentese et al., 2006; Yamada et al., 2007; Biedert and Bachmann, 2009; Li et al., 2010; Cerveri et al., 2010; Van Haver et al., 2014a; Cerveri et al., 2014; Nelitz et al., 2014; Monk et al., 2014; Cerveri et al., 2016). However, two main issues make such quantitative assessment particularly controversial. First of all, the reliability of thresholds is contingent to anthropometric variability (e.g. size, age, race and gender). Secondly, as the severity of the pathology increases, the trochlear morphology progressively loses its link with the normal shape, making landmarks difficult to measure or even meaningless (Nelitz et al., 2014). In order to overcome landmark-based drawbacks, surface-based techniques were recently explored, which take the full geometric complexity of trochlear region into account (Biedert et al., 2011; Nelitz et al., 2013; Cerveri et al., 2014). Among different modeling approaches of three-dimensional (3D) surfaces, statistical shape models (SSM) have been used to represent the morphological variability spread into a dataset of shapes. This representation encodes information in terms of modes of variations (MoVs) that model global, regional and local morphological features. In biomechanics and orthopedic fields, SSM of bony shapes were exploited for modeling the human scapula and the humerus (Mutsvangwa et al., 2015), studying the human femoral cortex morphology (Zhang et al., 2016), modeling the relation between shape and functions in the spine (Hollenbeck et al., 2018), reconstructing the femur from sparse 3D data and X-ray images (Zheng et al., 2007; Zhu and Li, 2011; Baka et al., 2014; Cerveri et al., 2017), and reconstructing the distal femur and the proximal tibia to investigate the relationship between shape and function in the knee joint (Fitzpatrick et al., 2011). Recently, SSM of the distal femur that focused on the trochlear region were proposed to predict the anatomically correct femur shape for trochlear dysplasia patients (Albrecht et al., 2013) and to model trochlear abnormality for staging purpose (Van Haver et al., 2014a). In recent papers of our group, we addressed the relation between pathological and physiological variability in the trochlear region represented by SSM (Cerveri et al., 2016; Cerveri et al., 2018). However, the morphological relations between the trochlear abnormality and the other parts of the distal femur were not taken into consideration. In view of that, the aim of this study was to develop a statistical shape model of distal femur to capture the pathological variability of the trochlear region into specific modes of variation and to disclose how local trochlear degeneration can be related to alterations of the distal femur morphology globally and whether specific MoVs can be associated to mechanical characteristics of the knee.

2. Material and methods

A retrospective dataset of distal femur shapes, provided by Medacta International SA upon anonymization, was considered in this study. The dataset included 100 surfaces, reconstructed from planning CT knee scans acquired on a patient group aged 67 ± 10 years. At staging time, the patients reported localized knee pain and mechanical knee instability with different cartilage damages and bony deformations. Along with surface data, hip-knee-ankle alignment, femoral internal-external rotation and tibial slope data were available for each patients. All of them underwent either resurfacing or replacement surgery of the knee between 2014

[1] Morphological degeneration is traditionally quantified by values smaller than 3–5 mm.
[2] Morphological degeneration is quantified by values greater than 135–140°.
[3] Morphological degeneration is quantified by values smaller than 15°.
[4] Morphological degeneration is quantified by values different from 1.
[5] Morphological degeneration is quantified by values approaching or smaller than 1.

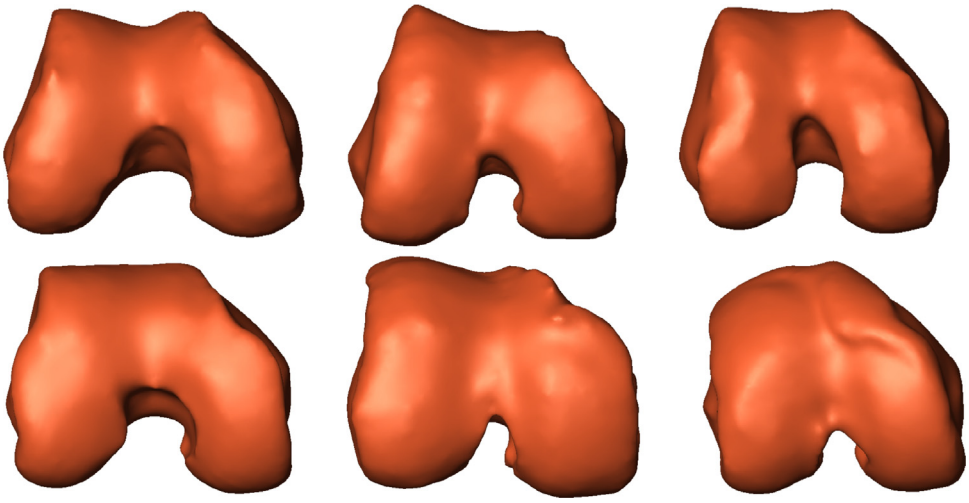

Fig. 2. Progressive degeneration of the trochlear region. A concurrent narrowing of the intercondylar notch, along with the enlargement of the condylar base, can be detected.

and 2016. About 520 axial slices were available for each scan, featuring image resolution and voxel size of 512×512 and $0.48 \times 0.48 \times 0.5$ mm, respectively. Expert radiology operators manually segmented the osseous portion of the distal femur, approximately up to 2–4 cm away from frontal notch of the trochlear region along the femur shaft, depending on the specific centering of the knee joint in the CT scan. Within the overall dataset, 42 cases were selected for SSM construction whereas the remaining were excluded because of large abnormalities at the condylar regions both posteriorly and laterally, induced by osteophytes, producing also deformations in the trochlear region. For such cases, we assumed that the specific effect of the morphological deformation of the trochlear surface on knee biomechanics could be difficult to assess. In the useful dataset, the condition of the trochlear region was diagnosed by one radiology expert as low (16), moderate (13), and (13) severe degeneration according to clinical practice (Fig. 2). With no loss of generality, left femur shapes were mirrored in medio-lateral direction to obtain equivalent right distal femurs. All the femur shapes, described by a triangle mesh, were slightly smoothed and down-sampled to 10,000 vertices.

In order to visualize and analyze inter-subject shape variation, a statistical model was developed according to the implementation described in (Cerveri et al., 2017; Cerveri et al., 2018). A reference surface, selected in the training set considering an instance featuring very low deformations, was used to compute the pair-wise rigid alignment of all the surfaces. Afterwards, point correspondences were computed exploiting a state-of-the-art deformable registration algorithm (Myronenko and Song, 2010), improved by means of a robust procedure we previously developed for ensuring one-to-one matching (Cerveri et al., 2018). Based on the mean model and the matrix difference, the covariance matrix was computed and processed by principal component analysis (PCA) attaining $M\text{-}1 = 41$ eigen-modes of variation (MoV). The SSM-based surface reconstruction is obtained by summing up the mean model $\overline{m}$ with the series of all MoVs (see Appendix A.1). In the second test, the quality of the SSM was assessed by quantifying the specificity as a function of the number of used MoVs (see Appendix A.2). The third analysis was focused on the description of the qualitative relation between the MoVs and the trochlear region. The role of each MoV was first quantified by means of the explained variance (EV), which represents the percentage amount of morphological variation, spread into the dataset, encoded by the *jth* MoV assuming that altogether the MoVs encode the overall 100% of variation (see Appendix A.3). Perturbations of ± 2 standard deviations from the mean of each MoV, approximating 95.5% of the variation in that MoV for the sample, were applied to each relevant MoV to visualize the changes in size, shape, and related morphological interactions among regions of the distal femur. The first H MoVs ($H < M$) with explained variances adding to 90% were used to reconstruct the surfaces assessing a median error (surface distance between the reconstructed and training instance) of 3.06 (IR: 0.75 mm) across the dataset. The fourth test was focused on the quantification of the relation between the most relevant MoVs and the trochlear parameters, along with the trochlear interplay with the condylar shapes. This test was based on the manual detection on the mean model of the same nine points described earlier. The correlation and the interplay was studied by morphing the mean model, one MoV at a time, using 50 equally spaced samples in the $[-2, +2]$ range of the corresponding $\{\lambda\}$ value (see Eq. (1)). For each morphed surface, the nine points were automatically obtained exploiting the indices of the corresponding vertices on the mean model so that the eight morphometric parameters were computed. Considering one MoV, the parameter p_i (e.g. TD) and the 50 morphed surfaces, the vector $p_{i,j}$, where j ranged between 1 and 50, was computed. The relation between each vector and the corresponding reference vector $\overline{p}_{i,j}$ was computed by means of the coefficient of determination (see Appendix A.4). The last test addressed the relation between MoVs and the mechanical stability of knee considering angular parameters as the alignment of the hip-knee-ankle mechanical axis (HKA), measured on the frontal plane, the internal external rotation of the femur with respect to the tibia (IER), measured on the axial plane, and the tibial slope (TS), measured on the sagittal plane. The biomechanical condition of the knee was evaluated by means of the physiological ranges of HKA ($\pm 3^\circ$), IER ($\pm 5^\circ$) and TS (from 2° to 6°). Such thresholds are traditionally used to discriminate between stability and instability of the knee. Each of the three indexes was assessed for all the patients using the planning images. Thus, we split the dataset in two classes, namely physiological and pathological conditions, according to the above mentioned ranges. We analyzed whether there was any statistical difference in the distribution of each SSM parameter across the physiological and pathological conditions for each biomechanical index (HKA, IER and TS). To the aim, the Wilcoxon rank sum test for equal medians ($p < 5\%$) was performed.

3. Results

The evaluation of TD, SA, LTI, TFAR and TAPR distributions across the dataset provided median values of 5.6 mm (IR: 1.95), 148.5° (IR: 10.3), 10.1° (IR: 17.0), 0.89 (IR: 0.16) and 0.97 (IR: 0.08), respectively (Fig. 3). These values indicated a general quantitative agreement of the dataset staged in the three progressive degeneration levels of the trochlear region. The ranges of ICN, LCS and MCS were about 14–21 mm, 22–32 mm, and 25–32 mm, respectively.

The specificity of the SSM, computed for five different EVs (70, 80, 90, 95 and 99%), showed median errors, lower than 2 mm, and similar IR ranges of about 0.5 mm (Fig. 4). This demonstrated the good quality of the implemented procedure to build the SSM. The evaluation of the single MoVs shed light on the morphological variations of the pathological distal femur set considered in this study. As expected the most relevant MoV pertained to the isotropic scale that accounted for more than 42% of the total variability across the surfaces in the dataset. The second one mainly encoded the height of the femoral shaft (Table 1) with EV = 16.9%. As far as the trochlear region is concerned, we found that the MoV #3 (EV = 7.7%) represented mainly variations of the trochlear region. The negative and positive ranges of the corresponding morphing parameter accounted for anterior sharpening and posterior flatting of the condylar facets, respectively (Fig. 5). This qualitative relation was in nice agreement with the computed correlations with TD, SA, LTI and TFAR parameters (Table 2). Relevant interplay was also detected with ICN, quantified by a high correlation (r^2: 0.71). From the corresponding LCS and MCS correlation results, the ICN shrinkage was mainly associated to a variation of the medial condylar size. For MoV #4 (EV = 6.2%), good correlation with both TD and SA was found. Visually, the MoV represented the medio-lateral size of trochlea area with shrinkage and enlargement encoded by negative and positive range of the morphing parameter. Quantitatively, this was in agreement with the low correlation found for TFAR (r^2: 0.18). Interestingly, this MoV also represented the height of the medial facet in anterior direction. Height reduction of the medial facet, usually reported as medial hypoplasia, is another morphological evidence of the trochlear degeneration, usually quantified by means of the TAPR. High interplay was detected with both the condylar sizes LCS (r^2: 0.67) and MCS (r^2: 0.99), meaning that the narrowing of the ICN was concurrent with a variation (width increase) of the two condylar bases (Fig. 5). The variability of depth of trochlear sulcus was again represented by MoV #5

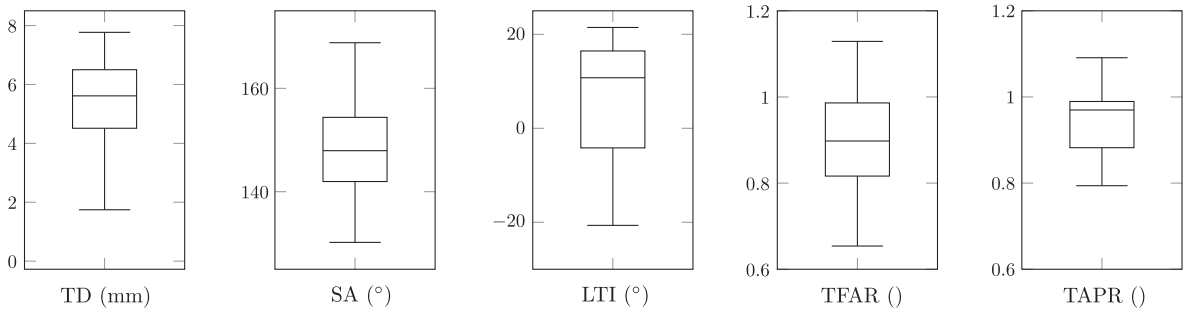

Fig. 3. Trochlear depth, sulcus angle, lateral trochlear inclination, trochlear facet asymmetry ratio and trochlear anterior- posterio ratio.

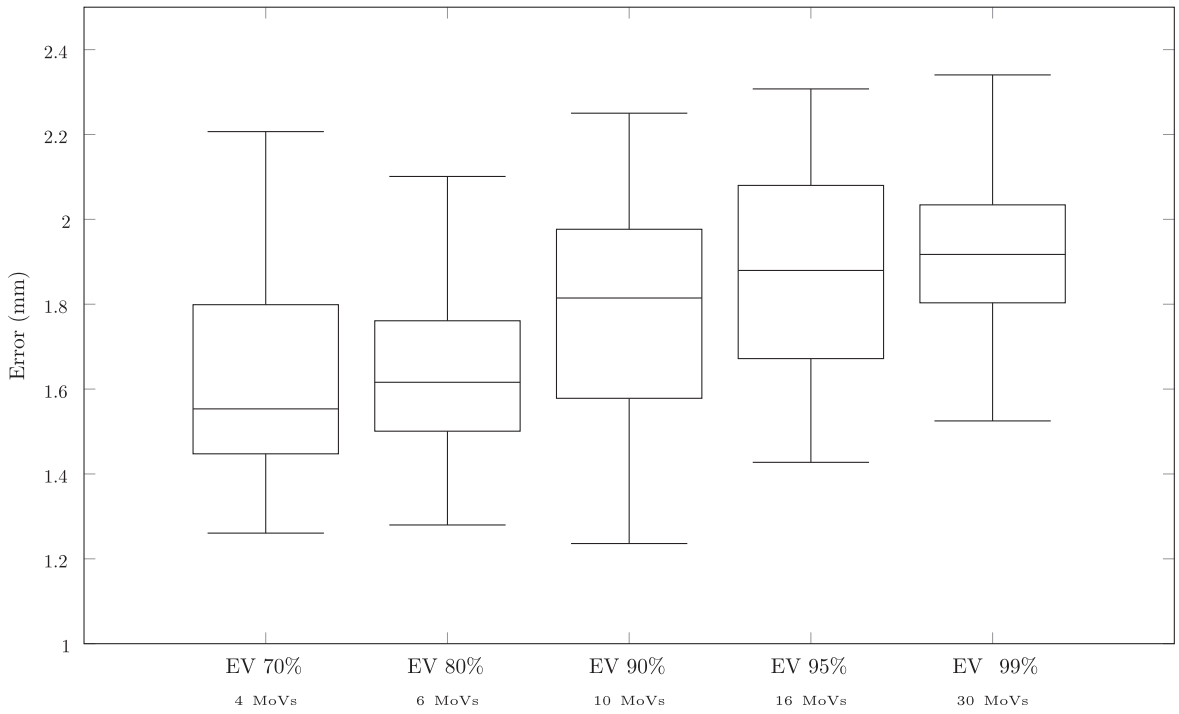

Fig. 4. Specificity as a function of the number of used MoVs.

Table 1
The first 10 MoVs explaining more than 90% of the morphological variability in the training dataset.

MoV	EV%	Transform/Region	Negative	Positive	Interplay
#1	42.7	Global scale	shrinkage	magnification	none
#2	16.9	Shaft length	elongation	shortening	none
#3	7.7	Trochlea	sharpen	flat	condylar notch
#4	6.2	Trochlea	shrinkage	enlargement	condylar notch
#5	4.3	Trochlea	flat	sharpen	medial condyle
#6	3.3	Axial rotation	extra	intra	medial condyle
#7	3.1	Trochlea	squeezing	enlargement	lateral condyle
#8	2.4	Shaft bending	posterior	anterior	condylar size
#9	2.3	Lateral facet	posterior	anterior	condylar notch
#10	1.3	Medial facet	posterior	anterior	medial condyle

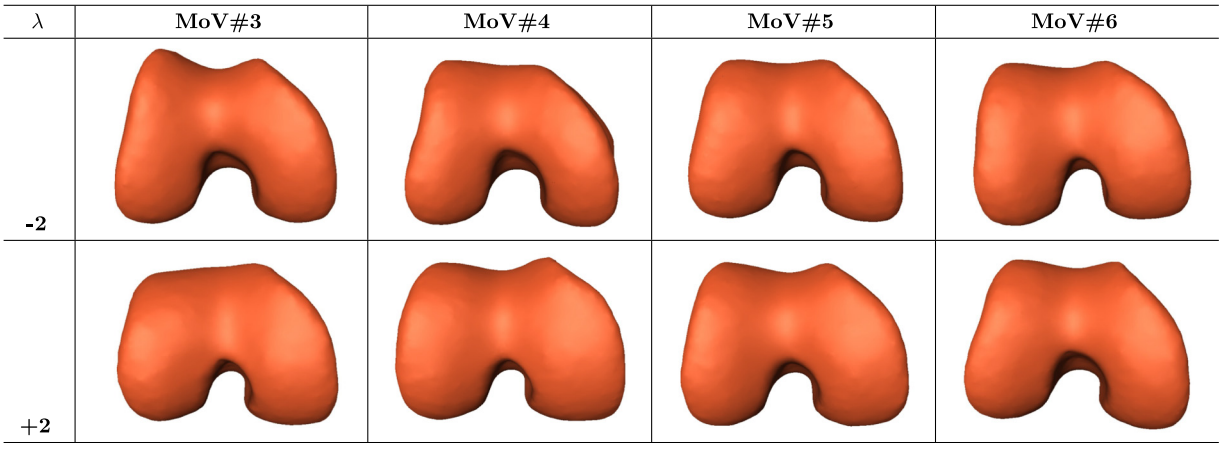

Fig. 5. Morphing surfaces of the first 4 MoVs depicting the morphological effects at the trochlear region.

Table 2
Correlation between relevant MoVs and quantitative parameters. MoVs #3, #4 and #7 feature the highest correlation with the morphometric parameters of the trochlea.

MoV	TD	SA	LTI	TFAR	TAPR	ICN	LCS	MCS
#3	0.70	0.70	0.66	0.70	0.48	0.71	0.12	0.54
#4	0.76	0.64	0.10	0.18	0.24	0.49	0.67	0.99
#5	0.53	0.46	0.24	0.38	0.01	0.09	0.52	0.71
#6	0.08	0.05	0.07	0.28	0.14	0.55	0.26	0.22
#7	0.65	0.65	0.58	0.55	0.40	0.76	0.42	0.66
#8	0.17	0.16	0.10	0.18	0.04	0.02	0.46	0.76
#9	0.20	0.17	0.35	0.02	0.35	0.53	0.64	0.26
#10	0.11	0.09	0.01	0.18	0.07	0.17	0.21	0.01

(EV = 4.3%), whose morphing parameter featured a positive/negative relation in opposition to that one of MoV #3. Interplay was less relevant with the intercondylar notch, however a concurrent enlargement of the medial condylar base was encoded (r^2: 0.71). MoV #6 (EV = 3.3%) represented the axial rotation that is usually a physiological parameter of the distal femur. As a matter of fact, the trochlear region was little affected and some interplay was found with the ICN only. MoV #7 (EV = 3.1%) mainly represented the anterior-posterior height of the lateral facet (Fig. 6), affecting less the medial facet. Quantitatively, a good correlation with TD and SA was detected. This MoV predicted the association between the increase of the prominence of the lateral facet (healthy condition) and the narrowing of the intercondylar notch (degenerative condition), along with the increase of the medial condylar base. Interestingly, this interplay was barely present in the training dataset. MoVs #8, #9 and #10 all were less related to the trochlear modifications (Table 2). MoV #8 mainly encoded the bending of the femur shaft in the sagittal plane predicting a partial interplay with the condylar sizes. MoV #9 was related to a partial lateralization of the lateral facet and predicted an interplay with the intercondylar notch width and the lateral condylar size. MoV #10 represented the variation of the medial facet in anterior-posterior direction with an interplay with the medial condylar width. Synthetically, MoVs #3, #4 and #7 featured the highest correlation with the morphometric parameters of the trochlea. Results of the last test showed that MoV #7 ($p = 0.02$) and #11 ($p = 0.03$) were statistically different in case of physiological and pathological conditions of the HKA. For IER and TS, we found that MoV #7 ($p = 0.01$) and #11 ($p = 0.02$), respectively, discriminated the two conditions.

4. Discussion and conclusions

In this paper, the SSM approach to shape analysis was proposed for describing and visualizing the abnormal morphology of the trochlear region in the distal femur. The main outcomes of the performed study can be summarized as follows. While built upon femur surfaces featuring wide shape heterogeneity, the SSM showed high specificity confirming the value of the adopted methods to compute accurate surface registration and robust point

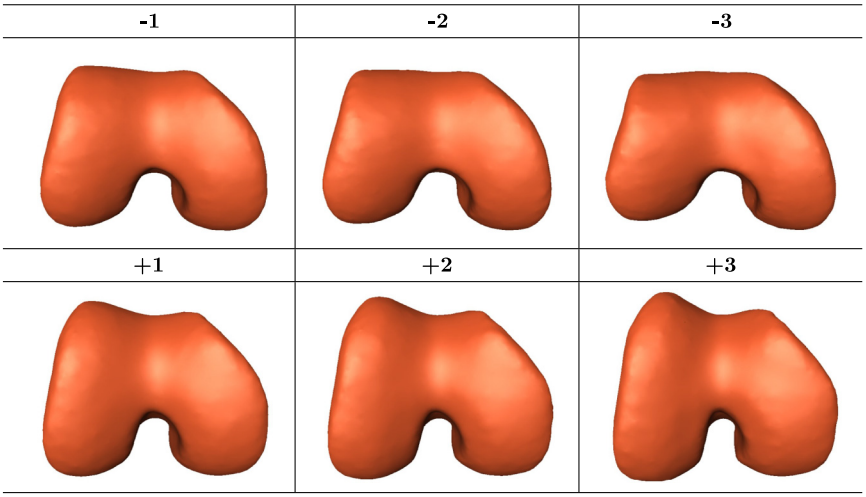

Fig. 6. Mov #7. Interplay between the trochlear region and the intercondylar notch width.

correspondence (Cerveri et al., 2017), which ensured the representation of the main morphological variability in the distal femur dataset. The SSM analysis allowed to identify MoVs specific for the trochlear geometry in agreement with the previous literature (Van Haver et al., 2014b; Iranpour et al., 2017; Cerveri et al., 2018). Apart from the first two MoVs, which encoded the global shape magnitude and femur shaft elongation in the axial direction, three MoVs, namely #3, #4 and #7, markedly embedded the morphological variations of the trochlea, as the depth of the groove and the shape of the condylar facets in anterior and distal directions. This particular finding was in agreement with the healthy/dysplastic classification based on SSM reported in Van Haver et al. (2014b). Correlation results in the range of 70% agreed with considerations arisen from the visual inspection thus enforcing the direct relation of relevant MoVs with the quantitative descriptors of the trochlear geometry. While testing the generalization of the SSM was beyond the scope of the work, SSM was able to generate femur shapes that were quite different from those included in the training dataset. For example, despite being uncommon, the association between the increase in the anterior direction of the lateral facet height and the narrowing of the intercondylar notch was encoded by one specific MoV (see Fig. 6). More in general, our findings confirmed the existence of many different interactions among trochlear and condylar deformations in agreement with previous reports in the literature (Yamada et al., 2007; Pedoia et al., 2015).

The reason of the adoption of the SSM approach to the morphological evaluation of trochlear region was twofold. First, it allowed to take into account its full geometry with respect to the traditional methods, based on 2D images, utilized to assess the clinical condition of the patello-femoral joint (Dejour et al., 1994; Merchant, 1988; Pfirrmann et al., 2000; Carrillon et al., 2000). Second, SSM offered the opportunity of performing an extensive visual analysis, as we shown, and being used as a computer-based tool to shed light on concurrent morphological variations (Fitzpatrick et al., 2011; Shi et al., 2014; Baka et al., 2014; Schneider et al., 2015). As far as traditional assessment methods are concerned, both qualitative and quantitative techniques have been recently criticized (Lippacher et al., 2012; Van Haver et al., 2014a; Nelitz et al., 2014; Cerveri et al., 2016; Dornacher et al., 2017; Pennock et al., 2018) because of the large uncertainty of the sign interpretation and the poor reliability of both landmarks and cut-off values, respectively. Especially, in the clinical evaluation of the trochlear dysplasia, quantitative measurements have been shown (Nelitz et al., 2014; Dornacher et al., 2017) very little correlated to the traditional 4-grade Dejour classification (Dejour et al., 1994). The present study was performed on a surface dataset of pathological femurs considering low, intermediate and severe degeneration of the trochlear morphology. While the landmark-based parameters are not completely reliable and group-specific, our analysis showed distribution of values coherent with the three considered classes (low, moderate, severe degeneration). In (Pfirrmann et al., 2000) for instance, the authors reported a cut-off of 3 mm for TD to discriminate between healthy and pathological trochlear conditions. They also found a median value of SA in the normality group of about 145° that however was greater that the normality reference values (138° and 140°) reported in (Merchant, 1988 and Davies et al., 2000), respectively. Similarly, the cut-off of 145° for SA (Dejour et al., 1994) turned out to be a very uncertain threshold, sensibly larger than the normality reference value (138°) previously reported in (Merchant, 1988). As far as LTI is concerned, Escala et al. (2006) found a cut-off of 14°, basically in agreement with that found by Nelitz et al. (2014) but quite different from that proposed by Carrillon et al. (2000) who reported that 11° was an excellent cut-off for discriminating healthy to pathological trochlear geometries. For our dataset that included both low and severe trochlear deformations, the LTI distribution spanned a wide range including positive values greater than 15° and even negative values (complete lateral facet flattening) (see Fig. 3).

As far as morphological correlations in the regions of knee bones, only recently some studies have attempted to investigate interactions between the trochlear geometry and distal femur shape, information that shed light on the biomechanics of both patello- and tibio-femoral knee joints (Fitzpatrick et al., 2011; Botchu et al., 2013b; Monk et al., 2014; Frosch et al., 2014; Van Haver et al., 2015; Smoger et al., 2015; Pedoia et al., 2015; Iranpour et al., 2017; Vercruysse et al., 2017), support better understanding of knee osteoarthritis development (Jungmann et al., 2013), outline morphological risk factors for disease progression (Botchu et al., 2013a; Pedoia et al., 2015) and provide new concepts for implant design (Dejour et al., 2014; Du et al., 2017). In this domain, a morphometric study on femoral geometries of healthy subjects concluded that the position of the trochlea is quite variable with respect to the condylar geometry, while the curvature of the trochlear groove was acknowledged to be predictive of the sagittal radius of the condyles (Monk et al., 2014). VanHaver et al. tailored a cadaver study to investigate the effect of severe trochlear abnormalities on the patello-femoral biomechanics. The authors reported sensible increase of internal rotation and lateral translation of the joint, arguing also that altered trochlear shape can affect the overall stability of the knee (Van Haver et al.,

2015). Fitzpatrick et al. (2011) developed a SSM of the patello- and tibio-femoral articular surfaces reporting that one of the first relevant MoVs encoded the depth of the sulcus groove. Similarly, Smoger et al. (2015) proposed a statistical model to characterize relationships between knee anatomy and kinematics, emphasizing the role of a subset of MoVs that encoded the morphological relation between the patella and the trochlea shapes. The role of the width of the intercondylar notch, with regard to the overall femoral morphology, was investigated by Pedoia et al. (2015) by means of SSM. The authors reported in particular a positive correlation between the decrease of the width and the increase of the risk for anterior cruciate ligament injuries. Trochlear shape variation was correlated with changes in the patello-femoral kinematics as reported in one very recent study (Iranpour et al., 2017) where the authors quantitatively assessed the relation between trochlear geometry and kinematics alterations by testing cadaver knee joints. Significant correlation was found between the sulcus and medial facet angle with medial stability. The relation between the condylar geometry and the morphology of the trochlear groove was recently investigate in healthy knees (Du et al., 2017), concluding that at increasing flatness of the condylar bases corresponded a reduction of the sulcus depth, similar to our findings. The comparative analysis of the distribution of the three biomechanical angular indices (HKA, IER and TS) suggested that some SSM parameters of the distal femur may discriminate between stability and instability of the knee. In particular, we found that MoV #7, which mostly encoded the posterior height of the lateral condyle, and MoV #11, which encoded the distal height of the medial condyle, appeared to account for instability due to HKA misalignment. Interestingly, MoV #7 also was found to suggest a relation with the potential knee instability due to abnormal IER. Similarly, MoV #11 played a role for the pathological condition of the tibial slope. While indirect, the relation of the femoral geometry with the tibial mechanics is actually reasonable since tibial slope, particularly among knees with misalignment, may be an important risk factor for incident accelerated knee osteoarthritis (Driban et al., 2016).

In conclusion, this paper contributes to strengthen the growing interest about the translation in clinics of SSM as innovative tools to visualize and quantify morphological variations of bony regions for diagnostic purposes. Particularly, the contribution is threefold. First, we showed how the statistical shape model of the distal knee can encode the patient geometry in terms of a set of relevant parameters (MoVs), which can be used to support the clinical decision in the staging of the trochlear abnormality. Second, we bought to the attention the role of the morphological interplay as a potential mechanism to infer both biomechanical and clinical effects, as for instance the specific case of the flatness of the trochlear region which was shown to be associated to the narrowing of the intercondylar notch, this being a risk factor for knee ligaments. Third, we highlighted the possibility of the statistical shape model to predict morphological associations not present in the original dataset used to compute the model. This feature discloses the opportunity of using SSM in advanced modeling environments to study how correlated shape changes in the bony geometries could affect the knee stability and potentially the kinematics as we found for some specific MOVs.

Ethical background

The study involved retrospective anonymized digital data provided by Medacta International SA (CH) in accordance with institutional ethical committee.

Declaration of Competing Interest

No party having a direct interest in the results of the research supporting this article has or will confer a benefit on the author (s) or on any organization with which the author(s) is/are associated.

Acknowledgments

We would like to thank Medacta International SA for providing patient data.

Appendix A. Supplementary material

Supplementary data associated with this article can be found, in the online version, at https://doi.org/10.1016/j.jbiomech.2019.07.008.

References

Albrecht, T., Lthi, M., Gerig, T., Vetter, T., 2013. Posterior shape models. Med. Image Anal. 17, 959–973. https://doi.org/10.1016/j.media.2013.05.010.

Baka, N., Kaptein, B.L., Giphart, J.E., Staring, M., de Bruijne, M., Lelieveldt, B.P.F., Valstar, E., 2014. Evaluation of automated statistical shape model based knee kinematics from biplane fluoroscopy. J. Biomech. 47, 122–129. https://doi.org/10.1016/j.jbiomech.2013.09.022.

Balcarek, P., Terwey, A., Jung, K., Walde, T.A., Frosch, S., Schttrumpf, J.P., Wachowski, M.M., Dathe, H., Strmer, K.M., 2013. Influence of tibial slope asymmetry on femoral rotation in patients with lateral patellar instability. Knee Surg. Sports Traumatol. Arthroscopy: Off. J. ESSKA 21, 2155–2163. https://doi.org/10.1007/s00167-012-2247-4.

Biedert, R.M., Bachmann, M., 2009. Anterior-posterior trochlear measurements of normal and dysplastic trochlea by axial magnetic resonance imaging. Knee Surg. Sports Traumatol. Arthroscopy: Off. J. ESSKA 17, 1225–1230. https://doi.org/10.1007/s00167-009-0824-y.

Biedert, R., Sigg, A., Gal, I., Gerber, H., 2011. 3d representation of the surface topography of normal and dysplastic trochlea using mri. Knee 18, 340–346. https://doi.org/10.1016/j.knee.2010.07.006.

Botchu, R., Obaid, H., Rennie, W.J., 2013a. Correlation between trochlear dysplasia and anterior cruciate ligament injury. Journal of orthopaedic surgery (Hong Kong) 21, 185–188. https://doi.org/10.1177/230949901302100214.

Botchu, R., Obaid, H., Rennie, W.J., 2013b. Correlation between trochlear dysplasia and the notch index. J. Orthop. Surg. (Hong Kong) 21, 290–293. https://doi.org/10.1177/230949901302100305.

Carrillon, Y., Abidi, H., Dejour, D., Fantino, O., Moyen, B., Tran-Minh, V.A., 2000. Patellar instability: assessment on mr images by measuring the lateral trochlear inclination-initial experience. Radiology 216, 582–585. https://doi.org/10.1148/radiology.216.2.r00au07582.

Cerveri, P., Marchente, M., Bartels, W., Corten, K., Simon, J.-P., Manzotti, A., 2010. Automated method for computing the morphological and clinical parameters of the proximal femur using heuristic modeling techniques. Ann. Biomed. Eng. 38, 1752–1766. https://doi.org/10.1007/s10439-010-9965-x.

Cerveri, P., Manzotti, A., Vanzulli, A., Baroni, G., 2014. Local shape similarity and mean-shift curvature for deformable surface mapping of anatomical structures. IEEE Trans. Bio-med. Eng. 61, 16–24. https://doi.org/10.1109/TBME.2013.2274672.

Cerveri, P., Baroni, G., Confalonieri, N., Manzotti, A., 2016. Patient-specific modeling of the trochlear morphologic anomalies by means of hyperbolic paraboloids. Comput. Assist. Surg. (Abingdon, England) 21, 29–38. https://doi.org/10.1080/24699322.2016.1178330.

Cerveri, P., Sacco, C., Olgiati, G., Manzotti, A., Baroni, G., 2017. 2d/3d reconstruction of the distal femur using statistical shape models addressing personalized surgical instruments in knee arthroplasty: a feasibility analysis. Int. J. Med. Robot. Comput. Assist. Surg. MRCAS 13. https://doi.org/10.1002/rcs.1823.

Cerveri, P., Belfatto, A., Baroni, G., Manzotti, A., 2018. Stacked sparse autoencoder networks and statistical shape models for automatic staging of distal femur trochlear dysplasia. Int. J. Med. Robot. Comput. Assist. Surg. MRCAS 14. https://doi.org/10.1002/rcs.1947. e1947.

Chen, S., Du, Z., Yan, M., Yue, B., Wang, Y., 2017. Morphological classification of the femoral trochlear groove based on a quantitative measurement of computed tomographic models. Knee Surg. Sports Traumatol. Arthroscopy: Off. J. ESSKA 25, 3163–3170. https://doi.org/10.1007/s00167-016-4236-5.

Cho, J.C.S., Haun, D.W., Morrell, A.P., Kettner, N.W., 2009. Patellar dislocation in a 16-year-old athlete with femoral trochlear dysplasia. J. Manip. Physiol. Therap. 32, 687–694. https://doi.org/10.1016/j.jmpt.2009.08.020.

Davidson, P.A., Rivenburgh, D., 2008. Focal anatomic patellofemoral inlay resurfacing: theoretic basis, surgical technique, and case reports. Orthop. Clin. North Am. 39 (337–46), vi. https://doi.org/10.1016/j.ocl.2008.02.003.

Davies, A.P., Costa, M.L., Shepstone, L., Glasgow, M.M., Donell, S., Donnell, S.T., 2000. The sulcus angle and malalignment of the extensor mechanism of the knee. J. Bone Joint Surg. Brit. 82, 1162–1166.

Dejour, H., Walch, G., Nove-Josserand, L., Guier, C., 1994. Factors of patellar instability: an anatomic radiographic study. Knee Surg. Sports Traumatol. Arthroscopy: Off. J. ESSKA 2, 19–26.

Dejour, D., Ntagiopoulos, P.G., Saffarini, M., 2014. Evidence of trochlear dysplasia in femoral component designs. Knee Surg. Sports Traumatol. Arthroscopy: Off. J. ESSKA 22, 2599–2607. https://doi.org/10.1007/s00167-012-2268-z.

de Lange-Brokaar, B.J.E., Bijsterbosch, J., Kornaat, P.R., Yusuf, E., Ioan-Facsinay, A., Zuurmond, A.-M., Kroon, H.M., Meulenbelt, I., Bloem, J.L., Kloppenburg, M., 2016. Radiographic progression of knee osteoarthritis is associated with mri abnormalities in both the patellofemoral and tibiofemoral joint. Osteoarthr. Cartilage 24, 473–479. https://doi.org/10.1016/j.joca.2015.09.021.

Dornacher, D., Trubrich, A., Guelke, J., Reichel, H., Kappe, T., 2017. Evaluation of a modified knee rotation angle in mri scans with and without trochlear dysplasia: a parameter independent of knee size and trochlear morphology. Knee Surg. Sports Traumatol. Arthroscopy: Off. J. ESSKA 25, 2447–2452. https://doi.org/10.1007/s00167-015-3919-7.

Driban, J.B., Stout, A.C., Duryea, J., Lo, G.H., Harvey, W.F., Price, L.L., Ward, R.J., Eaton, C.B., Barbe, M.F., Lu, B., McAlindon, T.E., 2016. Coronal tibial slope is associated with accelerated knee osteoarthritis: data from the osteoarthritis initiative. BMC BMC Musculoskelet. Disorders 17, 299. https://doi.org/10.1186/s12891-016-1158-9.

Du, Z., Chen, S., Yan, M., Yue, B., Zeng, Y., Wang, Y., 2017. Do size, shape, and alignment parameters of the femoral condyle affect the trochlear groove tracking? A morphometric study based on 3d- computed tomography models in chinese people. BMC Musculoskelet. Disorders 18, 4. https://doi.org/10.1186/s12891-016-1374-3.

Escala, J.S., Mellado, J.M., Olona, M., Gin, J., Saur, A., Neyret, P., 2006. Objective patellar instability: Mr-based quantitative assessment of potentially associated anatomical features. Knee Surg. Sports Traumatol. Arthroscopy: Off. J. ESSKA 14, 264–272. https://doi.org/10.1007/s00167-005-0668-z.

Fitzpatrick, C.K., Baldwin, M.A., Laz, P.J., FitzPatrick, D.P., Lerner, A.L., Rullkoetter, P. J., 2011. Development of a statistical shape model of the patellofemoral joint for investigating relationships between shape and function. J. Biomech. 44, 2446–2452. https://doi.org/10.1016/j.jbiomech.2011.06.025.

Frosch, S., Brodkorb, T., Schttrumpf, J.P., Wachowski, M.M., Walde, T.A., Strmer, K.M., Balcarek, P., 2014. Characteristics of femorotibial joint geometry in the trochlear dysplastic femur. J. Anat. 225, 367–373. https://doi.org/10.1111/joa.12214.

Fucentese, S.F., von Roll, A., Koch, P.P., Epari, D.R., Fuchs, B., Schottle, P.B., 2006. The patella morphology in trochlear dysplasia–a comparative mri study. Knee 13, 145–150. https://doi.org/10.1016/j.knee.2005.12.005.

Fucentese, S.F., Zingg, P.O., Schmitt, J., Pfirrmann, C.W.A., Meyer, D.C., Koch, P.P., 2011. Classification of trochlear dysplasia as predictor of clinical outcome after trochleoplasty. Knee Surg. Sports Traumatol. Arthroscopy: Off. J. ESSKA 19, 1655–1661. https://doi.org/10.1007/s00167-011-1410-7.

Gillespie, D., Mandziak, D., Howie, C., 2015. Influence of posterior lateral femoral condyle geometry on patellar dislocation. Arch. Orthop. Trauma Surg. 135, 1503–1509. https://doi.org/10.1007/s00402-015-2310-y.

Hing, C.B., Shepstone, L., Marshall, T., Donell, S.T., 2006. A laterally positioned concave trochlear groove prevents patellar dislocation. Clin. Orthop. Related Res. 447, 187–194. https://doi.org/10.1097/01.blo.0000203478.27044.9a.

Hollenbeck, J.F.M., Cain, C.M., Fattor, J.A., Rullkoetter, P.J., Laz, P.J., 2018. Statistical shape modeling characterizes three-dimensional shape and alignment variability in the lumbar spine. J. Biomech. 69, 146–155. https://doi.org/10.1016/j.jbiomech.2018.01.020.

Iranpour, F., Merican, A.M., Dandachli, W., Amis, A.A., Cobb, J.P., 2010. The geometry of the trochlear groove. Clin. Orthop. Related Res. 468, 782–788. https://doi.org/10.1007/s11999-009-1156-4.

Iranpour, F., Merican, A.M., Teo, S.H., Cobb, J.P., Amis, A.A., 2017. Femoral articular geometry and patellofemoral stability. Knee 24, 555–563. https://doi.org/10.1016/j.knee.2017.01.011.

Jungmann, P.M., Tham, S.-C., Liebl, H., Nevitt, M.C., McCulloch, C.E., Lynch, J., Link, T. M., 2013. Association of trochlear dysplasia with degenerative abnormalities in the knee: data from the osteoarthritis initiative. Skeletal Radiol. 42, 1383–1392. https://doi.org/10.1007/s00256-013-1664-x.

LaPrade, R.F., Cram, T.R., James, E.W., Rasmussen, M.T., 2014. Trochlear dysplasia and the role of trochleoplasty. Clin. Sports Med. 33, 531–545. https://doi.org/10.1016/j.csm.2014.03.005.

Latt, L.D., Christopher, M., Nicolini, A., Burk, D.R., Dezfuli, B., Serack, B.J., Fithian, D.C., 2014. A validated cadaveric model of trochlear dysplasia. Knee Surg. Sports Traumatol. Arthroscopy: Off. J. ESSKA 22, 2357–2363. https://doi.org/10.1007/s00167-014-3033-2.

Lee, T.Q., Morris, G., Csintalan, R.P., 2003. The influence of tibial and femoral rotation on patellofemoral contact area and pressure. J. Orthop. Sports Phys. Therapy 33, 686–693. https://doi.org/10.2519/jospt.2003.33.11.686.

Li, K., Tashman, S., Fu, F., Harner, C., Zhang, X., 2010. Automating analyses of the distal femur articular geometry based on three-dimensional surface data. Ann. Biomed. Eng. 38, 2928–2936. https://doi.org/10.1007/s10439-010-0064-9.

Lippacher, S., Dejour, D., Elsharkawi, M., Dornacher, D., Ring, C., Dreyhaupt, J., Reichel, H., Nelitz, M., 2012. Observer agreement on the dejour trochlear dysplasia classification: a comparison of true lateral radiographs and axial magnetic resonance images. Am. J. Sports Med. 40, 837–843. https://doi.org/10.1177/0363546511433028.

Longo, U.G., Vincenzo, C., Mannering, N., Ciuffreda, M., Salvatore, G., Berton, A., Denaro, V., 2017. Trochleoplasty techniques provide good clinical results in patients with trochlear dysplasia. Knee Surg. Sports Traumatol. Arthroscopy: Off. J. ESSKA. https://doi.org/10.1007/s00167-017-4584-9.

Merchant, A.C., 1988. Classification of patellofemoral disorders. Arthrosc. J. arthroscopic Related Surg. Off. Publ. Arthrosc. Assoc. North Am. Int. Arthrosc. Assoc. 4, 235–240.

Monk, A.P., Choji, K., O'Connor, J.J., Goodfellow, J.W., Murray, D.W., 2014. The shape of the distal femur: a geometrical study using mri. Bone Joint J. 96-B, 1623–1630. https://doi.org/10.1302/0301-620X.96B12.33964.

Mutsvangwa, T., Burdin, V., Schwartz, C., Roux, C., 2015. An automated statistical shape model developmental pipeline: application to the human scapula and humerus. IEEE Trans. Bio-med. Eng. 62, 1098–1107. https://doi.org/10.1109/TBME.2014.2368362.

Myronenko, A., Song, X., 2010. Point set registration: coherent point drift. IEEE Trans. Pattern Anal. Mach. Intell. 32, 2262–2275. https://doi.org/10.1109/TPAMI.2010.46.

Nelitz, M., Dreyhaupt, J., Lippacher, S., 2013. Combined trochleoplasty and medial patellofemoral ligament reconstruction for recurrent patellar dislocations in severe trochlear dysplasia: a minimum 2-year follow-up study. Am. J. Sports Med. 41, 1005–1012. https://doi.org/10.1177/0363546513478579.

Nelitz, M., Lippacher, S., Reichel, H., Dornacher, D., 2014. Evaluation of trochlear dysplasia using mri: correlation between the classification system of dejour and objective parameters of trochlear dysplasia. Knee Surg. Sports Traumatol. Arthroscopy: Off. J. ESSKA 22, 120–127. https://doi.org/10.1007/s00167-012-2321-y.

Pedoia, V., Lansdown, D.A., Zaid, M., McCulloch, C.E., Souza, R., Ma, C.B., Li, X., 2015. Three-dimensional mri-based statistical shape model and application to a cohort of knees with acute acl injury. Osteoarthr. Cartilage 23, 1695–1703. https://doi.org/10.1016/j.joca.2015.05.027.

Pennock, A.T., Chang, A., Doan, J., Bomar, J.D., Edmonds, E.W., 2018. 3d knee trochlear morphology assessment by magnetic resonance imaging in patients with normal and dysplastic trochleae. J. Pediatr. Orthop. https://doi.org/10.1097/BPO.0000000000001188.

Pfirrmann, C.W., Zanetti, M., Romero, J., Hodler, J., 2000. Femoral trochlear dysplasia: Mr findings. Radiology 216, 858–864. https://doi.org/10.1148/radiology.216.3.r00se38858.

Schneider, M.T.Y., Zhang, J., Crisco, J.J., Weiss, A.P.C., Ladd, A.L., Nielsen, P., Besier, T., 2015. Men and women have similarly shaped carpometacarpal joint bones. J. Biomech. 48, 3420–3426. https://doi.org/10.1016/j.jbiomech.2015.05.031.

Shi, X., Cao, L., Reed, M.P., Rupp, J.D., Hoff, C.N., Hu, J., 2014. A statistical human rib cage geometry model accounting for variations by age, sex, stature and body mass index. J. Biomech. 47, 2277–2285. https://doi.org/10.1016/j.jbiomech.2014.04.045.

Smoger, L.M., Fitzpatrick, C.K., Clary, C.W., Cyr, A.J., Maletsky, L.P., Rullkoetter, P.J., Laz, P.J., 2015. Statistical modeling to characterize relationships between knee anatomy and kinematics. J. orthop. Res. Off. Publ. Orthop. Res. Soc. 33, 1620–1630. https://doi.org/10.1002/jor.22948.

Song, G.-Y., Hong, L., Zhang, H., Zhang, J., Li, X., Li, Y., Feng, H., 2014. Trochleoplasty versus nontrochleoplasty procedures in treating patellar instability caused by severe trochlear dysplasia. Arthrosc. J. arthroscopic Related Surg. Off. Publ. Arthrosc. Assoc. North Am. Int. Arthrosc. Assoc. 30, 523–532. https://doi.org/10.1016/j.arthro.2014.01.011.

Van Haver, A., De Roo, K., De Beule, M., Van Cauter, S., Audenaert, E., Claessens, T., Verdonk, P., 2014a. Semi-automated landmark-based 3d analysis reveals new morphometric characteristics in the trochlear dysplastic femur. Knee Surg. Sports Traumatol. Arthroscopy: Off. J. ESSKA 22, 2698–2708. https://doi.org/10.1007/s00167-013-2573-1.

Van Haver, A., Mahieu, P., Claessens, T., Li, H., Pattyn, C., Verdonk, P., Audenaert, E.A., 2014b. A statistical shape model of trochlear dysplasia of the knee. Knee 21, 518–523. https://doi.org/10.1016/j.knee.2013.11.016.

Van Haver, A., De Roo, K., De Beule, M., Labey, L., De Baets, P., Dejour, D., Claessens, T., Verdonk, P., 2015. The effect of trochlear dysplasia on patellofemoral biomechanics: a cadaveric study with simulated trochlear deformities. Am. J. Sports Med. 43, 1354–1361. https://doi.org/10.1177/0363546515572143.

Vercruysse, C., Vandenneucker, H., Bellemans, J., Scheys, L., Luyckx, T., 2017. The shape and orientation of the trochlea run more parallel to the posterior condylar line than generally believed. Knee Surg. Sports Traumatol. Arthroscopy: Off. J. ESSKA. https://doi.org/10.1007/s00167-017-4685-5.

Yamada, Y., Toritsuka, Y., Yoshikawa, H., Sugamoto, K., Horibe, S., Shino, K., 2007. Morphological analysis of the femoral trochlea in patients with recurrent dislocation of the patella using three-dimensional computer models. J. Bone Joint Surg. Brit. 89, 746–751. https://doi.org/10.1302/0301-620X.89B6.18514.

Zhang, J., Fernandez, J., Hislop-Jambrich, J., Besier, T.F., 2016. Lower limb estimation from sparse landmarks using an articulated shape model. J. Biomech. 49, 3875–3881. https://doi.org/10.1016/j.jbiomech.2016.10.021.

Zheng, G., Dong, X., Rajamani, K.T., Zhang, X., Styner, M., Thoranaghatte, R.U., Nolte, L.-P., Ballester, M.A.G., 2007. Accurate and robust reconstruction of a surface model of the proximal femur from sparse-point data and a dense-point distribution model for surgical navigation. IEEE Trans. Bio-med. Eng. 54, 2109–2122.

Zhu, Z., Li, G., 2011. Construction of 3d human distal femoral surface models using a 3d statistical deformable model. J. Biomech. 44, 2362–2368. https://doi.org/10.1016/j.jbiomech.2011.07.006.